



## Research Article

Rajendran Selvamani\*, M. Mahaveer Sree Jayan, Rossana Dimitri, Francesco Tornabene, and Farzad Ebrahimi

# Nonlinear magneto-thermo-elastic vibration of mass sensor armchair carbon nanotube resting on an elastic substrate

<https://doi.org/10.1515/cls-2020-0012>

Received Jul 09, 2020; accepted Aug 23, 2020

**Abstract:** The present paper aims at studying the nonlinear ultrasonic waves in a magneto-thermo-elastic armchair single-walled (SW) carbon nanotube (CNT) with mass sensors resting on a polymer substrate. The analytical formulation accounts for small scale effects based on the Eringen's nonlocal elasticity theory. The mathematical model and its differential equations are solved theoretically in terms of dimensionless frequencies while assuming a nonlinear Winkler-Pasternak-type foundation. The solution is obtained by means of ultrasonic wave dispersion relations. A parametric work is carried out to check for the effect of the nonlocal scaling parameter, together with the magneto-mechanical loadings, the foundation parameters, the attached mass, boundary conditions and geometries, on the dimensionless frequency of nanotubes. The sensitivity of the mechanical response of nanotubes investigated herein, could be of great interest for design purposes in nano-engineering systems and devices.

**Keywords:** Nonlocal elasticity, Armchair, Mass sensor, CNT, Euler-beam theory, NEMS

## 1 Introduction

Magneto-thermo-elastic armchair single-walled (SW) carbon nanotubes (CNTs) represent an advanced material

largely adopted in many nanostructural applications. The application of  $\text{MnO}_2$ - $\text{FeTiO}_3$  (MFT)-based nanocomposites in a polymer matrix, as surrounding medium, has attracted the attention of the scientific community, due to the increased efficiency of embedded nanostructures [1]. Among nonlocal continuum theories, the nonlocal Euler-Bernoulli and Timoshenko beam models enable a satisfactory size-dependent assessment of CNTs, see Refs. [2, 3]. Some pioneering studies on the topic were presented by Eringen [4–6], who proposed some nonlocal continuum theories that were validated for different nanomaterials. Wang *et al.* [7] applied some nonlocal continuum models to investigate the size-dependent buckling response and vibration modes of CNTs.

Fang [8] applied a nonlocal elasticity theory to study the nonlinear free vibration of double walled CNTs. He found that the surrounding elastic medium plays a key role in the nonlinear propagation and amplitudes development. Saadatnia and Esmailzadeh [9] performed a systematic study of the nonlinear harmonic vibration of a piezoelectric-layered nanotube conveying fluid flow, while verifying the effect of the small scale parameters on the frequency response of the system in presence of fluid. In a further work, Askari and Esmailzadeh [10] investigated the forced vibration of fluid conveying CNTs, including the thermal effects and nonlinear foundations. Gheshlaghi and Hasheminejad [11] investigated the nonlinear vibrational behaviour of homogenous nanobeams and its dependence on the surface properties.

Sadeghi-Goughari *et al.* [12] studied the vibration response of a CNT conveying magnetic fluid under a longitudinal magnetic field. Similarly, Ya-Xin Zhena *et al.* [13] modeled the free vibration behaviour of viscoelastic nanotubes under a longitudinal magnetic field and verified the nonlocal parameter-dependence of the natural frequencies. Dai *et al.* [14] explored theoretically the postbuckling properties of nonlocal nanobeams in a longitudinal magnetic field. Ebrahimi and Barati [15] investigated the wave propagation in nonlocal porous multi-phase nano-crystalline nanobeams under a longitudinal

\*Corresponding Author: Rajendran Selvamani: Department of mathematics, Karunya Institute of Technology and Sciences, Coimabtoe, 641114, Tamilnadu, India;  
Email: selvamani@karunya.edu

M. Mahaveer Sree Jayan: Research scholar;  
Email: mahaveersreejayan@gmail.com

Rossana Dimitri, Francesco Tornabene: Department of Innovation Engineering, University of Salento, Lecce, Italy

Farzad Ebrahimi: Department of Mechanical Engineering, Imam Khomeini International University, Qazvin 34148-96818, Iran

magnetic field effect. They found that wave frequencies and phase velocities may increase or decrease with reduced inhomogeneity magnitudes. Li *et al.* [16] applied a nonlocal strain gradient theory to study the wave propagation in viscoelastic single-walled CNTs under a magnetic field, while checking for the sensitivity of the response to the surface properties and damping parameters. Arani *et al.* [17] discussed the longitudinal magnetic field effect on the wave propagation of fluid-conveyed SWCNTs using the Knudsen number and surface considerations. Zhang *et al.* [18] investigated the vibration of horn-shaped SWCNTs embedded in a viscoelastic medium under a longitudinal magnetic field. A two-scale coefficient model was developed by Güven [19] to study the propagation of longitudinal stress waves under a longitudinal magnetic field in a unified nonlocal elasticity context. Wang [20] validated the nonlocal elastic shell model for the study of longitudinal waves in SWCNTs and found that the microstructure and the coupling effect of the longitudinal wave and radial motion play a key role in the dispersion of waves. Azarboni [21] explored the magneto-thermal primary frequency response of CNTs, including the surface effect, under different boundary conditions. They inferred that an increased longitudinal magnetic field moves the backward jumping at higher excitation amplitudes, for different boundary conditions. Pradhan and Phadikar [22] applied a nonlocal continuum model to analyse the size-dependent vibration of embedded multi-layered graphene sheets.

The thermal buckling properties of zigzag SWCNTs were investigated by Semmah *et al.* [23], using a refined nonlocal model, while checking their dependence on the scale effect and chirality. Naceri *et al.* [24] investigated numerically the wave propagation in armchair SWCNTs under thermal conditions. Baghdadi *et al.* [25] proposed a nonlocal parabolic beam theory to analyze the thermo-mechanical vibration properties of armchair and zigzag SWCNTs. Based on a wide systematic numerical campaign, the authors verified a meaningful dependence of the natural frequencies on the temperature variation and chirality of armchair and zigzag CNTs. In a similar directions moves the work by Benzair *et al.* [26], where a nonlocal Timoshenko beam theory was employed to analyze the thermal sensitivity of SWCNTs, whose vibration response was compared to predictions based on a nonlocal Euler beam model. For further studies on the coupled vibration of CNTs based on a nonlocal elasticity, the reader is referred to [27–45].

In recent years, different studies on nanoscale structures coupled with mass sensors have been performed in literature [46–54]. More specifically, Wu *et al.* [46] analysed the resonance frequency of a SWCNT via a contin-

uum mechanics-based finite element method (FEM). Li and Chou [47] modeled the CNT nano-mass sensors with a molecular structural mechanics method. Another similar study was presented by Barati and Shahverdi [48] to examine the frequency shift behavior of plate-type nano-mass sensors made of FG nanostructures. The potential of SWCNTs as mass sensors was recently investigated by Chowdhury *et al.* [49] based on a continuum mechanics theory.

Arda and Aydogdu [50] analysed the vibration response of CNT mass sensors considering its sensitivity to the mass and stiffness ratios, along with the position of the detected elastic mass and nonlocal parameters. Similarly, Liu and Lyu [51] proposed a nonlocal strain gradient plate theory to model a novel nanoscale mass sensor made of a smart functionally-graded (FG) magneto-electro-elastic nanofilm integrated with graphene skins. In the further work by Lee *et al.* [52], the frequency equation of CNT-based cantilever sensors with an attached mass was derived theoretically using a nonlocal elasticity theory. Moreover, Nematollahi *et al.* [53] solved theoretically an inverse problem to determine the fluid velocity and mass ratio of a piezoelectric nanotube conveying fluid flow, according to the Eringen's nonlocal elasticity approach and the Euler–Bernoulli beam theory. Based on the same assumptions, Aydogdu and Filiz [54] performed a parametric analysis of the axial small-scale vibration behaviour of SWCNT-based mass sensors, considering the nonlocal effect together with the length of CNTs and the attached mass.

Based on the available literature, however, it seems that there is a general lack of studies focusing on the nonlinear ultrasonic waves in a magneto-thermo-elastic armchair SW-CNTs with mass sensors resting on polymer matrix. This is here proposed and analysed by means of a nonlocal Euler beam theory, in agreement with the Eringen's assumptions, in order to account for small scale effects. Thus, we determine the solutions of the ultrasonic wave dispersion relations governing the problem, whereby a parametric study is carried out systematically to check for the influence of the magneto-electro-mechanical loading, attached mass, nonlocal parameter, and aspect ratio, on the deflection properties of nanotubes.

## 2 Mathematical formulation

### 2.1 Eringen nonlocal theory of elasticity

Based on the Eringen's nonlocal theory of elasticity, we assume that the stress state at a reference point  $x$  in the body depends not only on the strain state at the same point  $x$ ,

but also on the strain states at all other points  $X'$  of the body. The general form of the constitutive equations in a nonlocal form contains an integral over the entire region of interest. The integral contains a non-local kernel function, which describes the relative influence of the strain field at various locations on the stress state at a given location. The constitutive equations of linear, homogeneous, isotropic, nonlocal elastic solid with zero body forces, are given by Eringen [4–6] as follows

$$\sigma_{ij} + \rho(f_j - \ddot{u}_j) = 0 \quad (1)$$

$$\sigma_{ij}(X) = \int_V \pi(|X - X'|, \tau) \sigma_{ij}^c(X') dv(X') \quad (2)$$

$$\sigma_{ij}^c = C_{ijkl} \varepsilon_{kl} \quad (3)$$

$$e_{ij}(X') = \frac{1}{2} (u_{i,j} + u_{j,i}) \quad (4)$$

Eq. (1) is the equilibrium equation, where  $\sigma_{ij}$ ,  $\rho$ ,  $f_j$ ,  $u_j$  refer to the stress tensor, mass density, body force density and displacement vector at a reference point  $x$  in the body, respectively, at time  $t$ . Eq. (3) is the classical constitutive relation where  $\sigma_{ij}^c(X')$  is the classical stress tensor at any point  $X'$  in the body, which is related to the linear strain tensor  $e_{ij}(X')$  at the same point. Eq. (4) refers to the classical kinematic relations. The kernel function  $\pi(|X - X'|, \tau)$  is the attenuation function which includes the nonlocal effect in the constitutive equations. The volume integral in Eq. (2) is defined over the volume  $V$  of the body. The nonlocal modulus in Eq. (2) has dimensions  $(length)^{-3}$  and it depends on a characteristic length (*i.e.* lattice parameter, size of grain, granular distance, etc.) and on the external characteristic length of the system  $l$  (*i.e.* wavelength, crack length, size or dimensions of sample, etc.). Therefore, the nonlocal modulus can be written in the following form

$$\pi = \pi(|X - X'|, \tau), \tau = \frac{e_0 a}{l} \quad (5)$$

where  $e_0 a$  is a constant parameter that must be determined for each material, independently. Then, the integro-partial differential Eq. (2) for a non-local elasticity problem can be simplified into a partial differential equation, as follows

$$(1 - \tau^2 l^2 \nabla^2) \sigma_{ij}(X) = \sigma_{ij}^c(X) = C_{ijkl} e_{kl}(X) \quad (6)$$

where  $C_{ijkl}$  is the elastic modulus tensor of a classical isotropic elasticity, and  $e_{ij}$  is the strain tensor;  $\nabla^2$  denotes the second-order spatial gradient applied on the stress tensor  $\sigma_{ij}$ , and  $\tau = e_0 a/l$ . In agreement with findings by

Eringen, we can consider  $e_0 = 0.39$  by matching the dispersion curves via a nonlocal theory for plane waves and born-Karman model of lattice dynamics at the end of the Brillouin zone ( $ka = \pi$ ), where  $a$  is the distance between atoms, and  $k$  is the wavenumber in a phonon analysis. On the other hand, Eringen [5] assumed  $e_0 = 0.31$  in his study for a Rayleigh surface wave, via a nonlocal continuum mechanics and lattice dynamics.

## 2.2 Atomic structure of CNTs

CNTs are tubes formed by rolling a graphene sheet about the  $\vec{T}$  vector. A vector perpendicular to the  $\vec{T}$  is the chiral vector denoted by  $\vec{C}_h$ . The chiral vector and corresponding chiral angle define the type of CNT. Zigzag, armchair and chiral  $\vec{C}_h$  can be expressed with respect to the base vectors  $\vec{a}_1$  and  $\vec{a}_2$  as follows

$$\vec{C}_h = n\vec{a}_1 + m\vec{a}_2 \quad (7)$$

where  $n$  and  $m$  are indices of translation that define the structure around the circumference. Figure 1 describes the lattice of transition  $(n, m)$  along with the base vectors  $\vec{a}_1$  and  $\vec{a}_2$ . If the indices of translation are such that  $m = 0$  and  $m = n$ , the CNT corresponds to a zigzag or armchair structure, respectively. The diameter of an armchair SW CNT for  $m = n$  is defined as [55]

$$d = \frac{3na}{\pi} \quad (8)$$

Based on the connection between molecular mechanics and solid mechanics, Wu *et al.* [56] developed an energy-equivalent model for studying the mechanical properties of SW CNT. Using the same method, the equivalent Young's modulus for an armchair nanotube is expressed as

$$E_{SWCNT} = \frac{4\sqrt{3}KC}{9Ct + 4Ka^2t(\gamma_{21}^2 + \gamma_{22}^2)} \quad (9)$$

where  $K$  and  $C$  are the force constants;  $t$  is the thickness; parameters  $\gamma_{21}$  and  $\gamma_{22}$  are defined as

$$\gamma_{21} = \frac{-3\sqrt{4} - 3\cos^2(\pi/2n) \cos(\pi/2n)}{8\sqrt{3} - 2\sqrt{3}\cos^2(\pi/2n)}$$

$$\gamma_{22} = \frac{12 - 9\cos^2(\pi/2n)}{16\sqrt{3} - 4\sqrt{3}\cos^2(\pi/2n)}$$

By assuming  $n \rightarrow \infty$ , the Young's modulus for a graphite sheet becomes as

$$E_g = \frac{16\sqrt{3}Kt}{18Ct + Ka^2t} \quad (10)$$

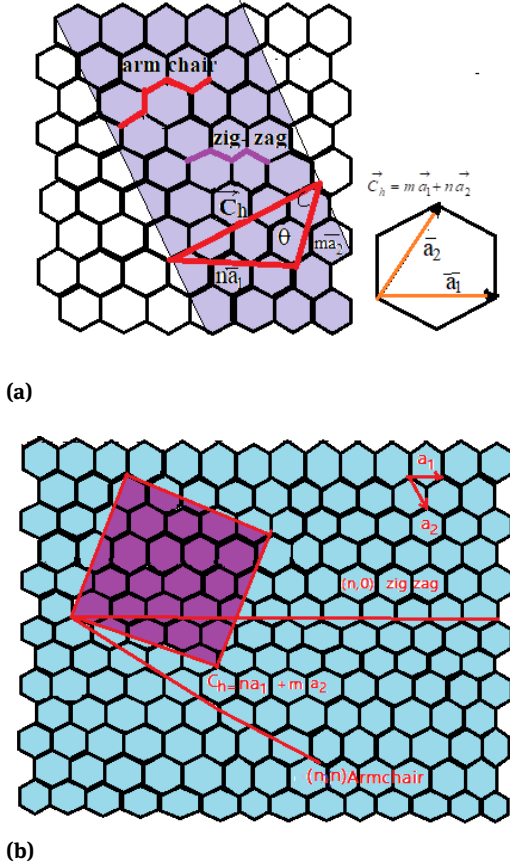


**Figure 1:** (a) Geometric properties of a SWCNT (b) Graphene structure for a CNT

### 2.3 Basic equations of the problem for a magnetic field force

CNTs appear in a hollow structure formed by covalently bonded carbon atoms, which can be imagined as a rectangular graphite sheet rolled from one side of its longest edge, to form a cylindrical tube (see Figure 2). A cylindrical coordinate system  $(X, \theta, Z)$  is shown in Figure 3, where  $X$  refers to the longitudinal direction of the shell,  $\theta$  defines its circumferential direction, and  $Z$  corresponds to the radial direction. This means that the surface defined by  $Z = 0$  is set on the middle surface of the shell. By assuming that the magnetic permeability,  $\eta$ , of CNTs equals the magnetic permeability of the surrounding medium, we can write the Maxwell equation as follows

$$f = \nabla \times \bar{s}, \quad \nabla \times \varepsilon = -\eta \cdot \frac{\partial \bar{s}}{\partial t}, \quad \text{div} \bar{s} = 0, \quad (11)$$

$$\bar{s} = \nabla \times (\bar{U} \times \bar{H}), \quad \varepsilon = -\eta \left( \frac{\partial \bar{s}}{\partial t} \times \bar{H} \right)$$

where  $f, \bar{s}, \varepsilon$  and  $\bar{U}$  represent the current density, strength vectors of electric field, disturbing vectors of magnetic

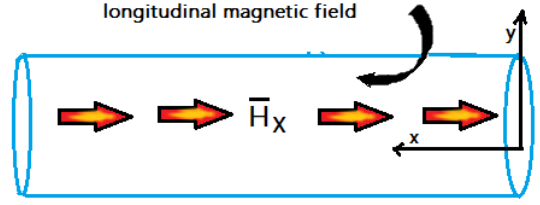


**Figure 2:** Single-walled carbon nanotube subjected to axial magnetic field

field and the vector of displacement respectively,  $\nabla$  is the Hamilton operators for shells  $\nabla = \left( \frac{\partial}{\partial X} \bar{i} + \frac{1}{R} + \frac{\partial}{\partial \theta} \bar{j} \right)$ . Applying a longitudinal magnetic field vector  $\bar{H}(H_x, 0, 0)$  on the  $i$ th layer CNT with the cylindrical coordinate  $(R, \theta, Z)$  and the displacement vector  $\bar{U} = (W_i, V_i, Y_i)$  of the  $i$ th layer CNT to Eq. (11), we get the following relations

$$\bar{s} = \nabla \times (\bar{U} \times \bar{H}) = \begin{pmatrix} -\frac{H_x}{R_i} \cdot \frac{\partial V_i}{\partial \theta}, \\ H_x \cdot \frac{\partial V_i}{\partial X}, \\ H_x \cdot \frac{\partial Y_i}{\partial X} \end{pmatrix} \quad (12a)$$

$$f = \nabla \times \bar{s} = \begin{pmatrix} \frac{H_x}{R_i} \cdot \frac{\partial^2 Y_i}{\partial X \partial \theta}, \\ -H_x \cdot \frac{\partial^2 Y_i}{\partial X^2}, \frac{H_x}{R_i^2} \cdot \frac{\partial^2 V_i}{\partial \theta^2} + H_x \cdot \frac{\partial^2 V_i}{\partial X^2} \end{pmatrix} \quad (12b)$$

The Lorentz force  $q$  induced by a longitudinal magnetic field can be written as

$$q(\bar{q}_X, \bar{q}_\theta, \bar{q}_Z) = f \times B \quad (12c)$$

$$= f \times \eta \bar{H} = \eta \left( 0, \frac{H_x^2}{R_i^2} \frac{\partial^2 V_i}{\partial X^2} + H_x^2 \cdot \frac{\partial^2 V_i}{\partial X^2}, H_x^2 \cdot \frac{\partial^2 Y_i}{\partial X^2} \right)$$

where  $\bar{q}_X, \bar{q}_\theta$  and  $\bar{q}_Z$  express the Lorentz force along the  $X, \theta$  and  $Z$  direction as follows (Figure 3)

$$\bar{q}_X = 0 \quad (12d)$$

$$\bar{q}_\theta = \eta \left( \frac{H_x^2}{R^2} \cdot \frac{\partial^2 V_i}{\partial X^2} + H_x^2 \cdot \frac{\partial^2 V_i}{\partial X^2} \right) \quad (12e)$$

$$\bar{q}_Z = \eta \left( H_x^2 \cdot \frac{\partial^2 Y_i}{\partial X^2} \right) \quad (12f)$$

The external force  $q_{mag}$  consists of the Lorentz force  $\bar{q}_Z$  due to the longitudinal magnetic field, and the distributed transverse force  $F_s$  due to the effect of surface tension, namely

$$q_{(mag)} = \bar{q}_Z(x) + F_s \quad (13)$$

where the Lorentz force  $\bar{q}_Z$  is defined by Eq. (12f), [16], and the distributed transverse force  $F_s$  can be defined as [51]

$$F_s = \left( H_s \cdot \frac{\partial^2 Y_i}{\partial X^2} \right) \quad (14)$$

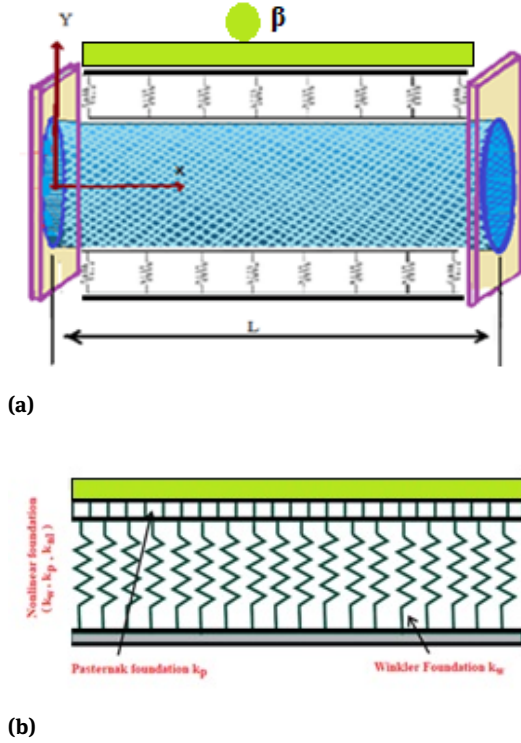


**Figure 3:** Geometry of SWCNT in (a) polymer matrix; (b) nonlinear foundation

Here,  $\eta$  is the magnetic permeability,  $H_x$  is the component of the longitudinal magnetic field vector exerted on the SWCNTs in the  $x$  direction, and  $H_s$  is a constant, defined as

$$H_s = 2\mu(d + h) \quad (15)$$

where  $\mu$  denotes the residual surface tension. The term  $\bar{q}_z$  is the magnetic force per unit length due to Lorentz force exerted on the tube in  $z$ -direction, where the effect bending stiffness  $EI$  is defined as [57, 58]

$$EI^* = EI + Q_s E_s \quad (16)$$

In the last relation,  $Q_s = \frac{\pi}{8}(d + h)^3$ ,  $E_s$  denotes the surface Young's modulus,  $h$  is the effective thickness of SWCNTs, and  $d$  is defined by Eq. (8).

### 3 Euler Bernoulli beam theory (EBT) based on nonlocal relations

The partial differential equation governing the free vibration of a nanotube under a thermal and Lorentz force can be expressed as

$$\frac{\partial \Pi}{\partial X} + N_t \frac{\partial^2 Y}{\partial X^2} + q_{(mag)} + \beta y + f(x) = \rho A \frac{\partial^2 Y}{\partial t^2} \quad (17)$$

where  $f(x)$  is the interaction pressure per unit axial length between the nanotube and the surrounding elastic medium;  $A$  is the cross section of CNT, and

$$\beta = \frac{f}{1 - \left(\frac{\alpha}{L^2}\right) f} \quad (18a)$$

$$f = \frac{m\omega^2 L^2}{EA}, \quad \alpha = \frac{M_p}{mL} \quad (18b)$$

where  $f$  is the non-dimensional frequency parameter,  $\alpha$  is the mass ratio (attached mass/mass of CNT),  $m$  is the mass per unit length according to a nonlocal elasticity approach. The resultant shear force  $\Pi$  on the cross section of the nanotube is defined as

$$\Pi = \frac{\partial M}{\partial X} \quad (19)$$

where  $N_t$  denotes the temperature-dependent axial force with thermal expansion coefficient  $\alpha$ . This constant force is defined as [59]

$$N_t = -EA\alpha T \quad (20)$$

where  $T$  is the temperature variable. The longitudinal magnetic flux due to a Lorentz force exerted on the tube in  $Z$ -direction is represented by  $q_z$ , which is defined as

$$q_z = \eta A H_x^2 \frac{\partial^2 Y}{\partial X^2} - EA\alpha T \quad (21)$$

being  $H_x$  the magnetic field strength and  $\eta$  the magnetic permeability. For the Euler-beam theory, the resultant bending moment  $M$  in Eq. (19) reads

$$M = \int_A z \sigma_{xx} dA \quad (22)$$

where  $\sigma_{xx}$  is the nonlocal axial stress defined by the nonlocal continuum theory. The constitutive Eq. (6) for a homogeneous isotropic elastic solid in a non-local form for one-dimensional nanotube gets the following form

$$\sigma_{xx} - (e_0 a)^2 \frac{\partial^2 \sigma_{xx}}{\partial X^2} = E \varepsilon_{xx} \quad (23)$$

where  $E$  is the Young's modulus of the tube,  $\varepsilon_{xx}$  is the axial strain,  $(e_0 a)$  is a nonlocal parameter;  $a$  is the internal characteristic length. The temperature-dependent nonlocal relations in Eq. (23) can be rewritten as

$$\sigma_{xx} - (e_0 a)^2 \frac{\partial^2 \sigma_{xx}}{\partial X^2} = E \varepsilon_{xx} - E \alpha T \quad (24)$$

According to a Euler –Bernoulli beam model, the axial strain  $\varepsilon_{xx}$  for small deflection is defined as

$$\varepsilon_{xx} = -z \frac{\partial^2 Y}{\partial X^2} \quad (25)$$

where  $z$  is the transverse coordinate in the positive direction of deflection. By combining Eqs. (24)-(25), with Eq. (22), the bending moment  $M$  can be expressed as

$$M - (e_0a)^2 \left[ \frac{\partial^2 M}{\partial X^2} \right] = EI^* \frac{\partial^2 Y}{\partial X^2} \quad (26)$$

where  $I = \int_A z^2 dA$  is the moment of inertia. By substituting Eq. (26) into Eq. (17), the nonlocal bending moment  $M$  and shear force  $\Pi$  become

$$M - (e_0a)^2 \left[ \frac{(\rho A) \frac{\partial^2 Y}{\partial t^2} + q_{(mag)}}{-f(x) + EA\alpha T} \right] = EI^* \frac{\partial^2 Y}{\partial X^2} \quad (27)$$

$$\Pi - (e_0a)^2 \left[ \frac{(\rho A) \frac{\partial^3 Y}{\partial X^2 \partial t^2} + \frac{\partial^2 q_{(mag)}}{\partial X^2}}{-\frac{\partial f(x)}{\partial X} + EA\alpha T} \right] = EI^* \frac{\partial^3 Y}{\partial X^3} \quad (28)$$

For the transverse vibration of the nanostructure under a distributed pressure and thermal interaction with the surrounding polymer elastic medium, the equation of motion (17) takes the following form

$$\begin{aligned} f(x) = & EI^* \frac{\partial^4 Y}{\partial X^4} + EA\alpha T \frac{\partial^2 Y}{\partial X^2} \\ & + (\beta + \rho A) \frac{\partial^2 Y}{\partial t^2} + q_{(mag)} \frac{\partial^2 Y}{\partial X^2} + F_s \frac{\partial^2 Y}{\partial X^2} \\ & - \left( (e_0a)^2 \left( \frac{EA\alpha T \frac{\partial^4 Y}{\partial X^4}}{+ \beta \frac{\partial^4 Y}{\partial X^2 \partial t^2} + q_{(mag)} \frac{\partial^4 Y}{\partial X^4}} \right) \right) \\ & + F_s \frac{\partial^4 Y}{\partial X^4} - \frac{\partial^2 f(x)}{\partial X^2} \end{aligned} \quad (29)$$

The pressure per unit axial length acting on the nanotube surface due to the surrounding elastic medium, can be described by a Winkler-Pasternak type model [59]

$$f(x) = -(-K_w + K_p + K_{nl}) \quad (30)$$

where  $K_w$ ,  $K_p$ ,  $K_{nl}$  refer to the Winkler, Pasternak and non-linear constant foundation. The introduction of Eq. (30) into Eq. (29) yields

$$\begin{aligned} EI^* \frac{\partial^4 Y}{\partial X^4} + EA\alpha T \frac{\partial^2 Y}{\partial X^2} + (\beta + \rho A) \frac{\partial^2 Y}{\partial t^2} \\ + \left( \eta AH_x^2 \frac{\partial^2 Y}{\partial X^2} + H_x \frac{\partial^2 Y}{\partial X^2} \right) \\ - (e_0a)^2 \left( \frac{EA\alpha T \frac{\partial^4 Y}{\partial X^4} + \rho A \frac{\partial^2 Y}{\partial X^2}}{+ \beta \frac{\partial^4 Y}{\partial X^2 \partial t^2} + q_{(mag)} \frac{\partial^4 Y}{\partial X^4}} \right) \\ + \left( \eta H_x^2 \frac{\partial^2 Y}{\partial X^2} - H_x \frac{\partial^4 Y}{\partial X^4} \right) \\ - (-K_w + K_p + K_{nl}) \frac{\partial^2 Y}{\partial X^2} \end{aligned} = -(-K_w + K_p + K_{nl}) \quad (31)$$

## 4 Ultrasonic wave solution

Eq. (29) can be transformed in a frequency domain using the Fourier transformation [60]

$$Y(x, t) = \sum_{n=1}^N \hat{Y}(x) e^{-j(kn - \omega_n t)} \quad (32)$$

where  $\hat{Y}$  is the amplitude of the wave motion,  $j = \sqrt{-1}$ ,  $k$  is the wave number,  $\omega_n$  the circular frequency of a sampling point, and  $N$  is the Nyquist frequency. The sampling rate and the number of sampling points should be sufficiently large to reach a good resolution for both high and low frequencies, respectively. By substitution of Eq. (32) into Eq. (30), we get

$$\begin{aligned} \left[ \left( EI^* \frac{\partial^4 \hat{Y}}{\partial X^4} + EA\alpha T \frac{\partial^2 \hat{Y}}{\partial X^2} + \left( \eta AH_x^2 \frac{\partial^2 \hat{Y}}{\partial X^2} + H_x \frac{\partial^2 \hat{Y}}{\partial X^2} \right) \right. \right. \\ \left. \left. + (\beta + \rho A) \frac{\partial^2 \hat{Y}}{\partial t^2} \right) \right. \\ \left. - (\tau)^2 \left( EA\alpha T \frac{\partial^2 \hat{Y}}{\partial X^2} + (\beta + \rho A) \frac{\partial^4 \hat{Y}}{\partial X^2 \partial t^2} - \left( \eta AH_x^2 \frac{\partial^2 \hat{Y}}{\partial X^2} \right) \right) \right. \\ \left. + H_x \frac{\partial^2 \hat{Y}}{\partial X^2} \right) - (-K_w + K_p + K_{nl}) \frac{\partial^2 \hat{Y}}{\partial X^2} \\ \left. + (-K_w + K_p + K_{nl}) \right] e^{i\omega_n t} = 0 \end{aligned} \quad (33)$$

This equation must be satisfied for each  $N$  and hence can be written as the ordinary differential equation in a single variable  $X$  as

$$\begin{aligned} \sum_{n=1}^N \left[ \left( EI^* \frac{\partial^4 \hat{Y}}{\partial X^4} + EA\alpha T \frac{\partial^2 \hat{Y}}{\partial X^2} + (\beta + \rho A) \frac{\partial^2 \hat{Y}}{\partial t^2} \right. \right. \\ \left. \left. + \left( \eta AH_x^2 \frac{\partial^2 \hat{Y}}{\partial X^2} + H_x \frac{\partial^2 \hat{Y}}{\partial X^2} \right) \right) \right. \\ \left. - (e_0a)^2 \left( \left( \beta + \rho A \right) \frac{\partial^4 \hat{Y}}{\partial X^2 \partial t^2} - \left( \eta AH_x^2 \frac{\partial^2 \hat{Y}}{\partial X^2} + H_x \frac{\partial^2 \hat{Y}}{\partial X^2} \right) \right) \right. \\ \left. - (-K_w + K_p + K_{nl}) \frac{\partial^2 \hat{Y}}{\partial X^2} + EA\alpha T \frac{\partial^2 \hat{Y}}{\partial X^2} \right) \\ \left. + (-K_w + K_p + K_{nl}) \right] e^{i\omega_n x} = 0 \end{aligned} \quad (34)$$

The last equation can be rewritten in terms of the single variable  $X$ , reducing as follows

$$\left[ \begin{aligned} & EI^* \frac{\partial^4 \hat{Y}}{\partial X^4} + EA\alpha T \frac{\partial^2 \hat{Y}}{\partial X^2} \\ & + \left( \eta AH_x^2 \frac{\partial^2 \hat{Y}}{\partial X^2} + H_x \frac{\partial^2 \hat{Y}}{\partial X^2} \right) - \frac{\partial^2}{\partial t^2} (\beta + \rho A) \\ & \left[ \begin{aligned} & \beta + \rho A - \\ & (-K_w + K_p + K_{nl}) + \\ & EA\alpha T \end{aligned} \right] \\ & \left( \eta AH_x^2 \frac{\partial^2 \hat{Y}}{\partial X^2} - \right) (\tau)^2 \frac{\partial^2 \hat{Y}}{\partial X^2} \\ & H_x \frac{\partial^2 \hat{Y}}{\partial X^2} \\ & + (-K_w + K_p + K_{nl}) \end{aligned} \right] = 0 \quad (35)$$

The dimensionless variables are defined as

$$\frac{X}{L} = x, \quad \frac{Y}{L} = y, \quad \alpha_i = \frac{I_i}{L}, \quad (36)$$

$$\tau = \frac{e_0 a}{l} \quad K_w = \frac{k_w L^4}{EI^*}, \quad K_p = \frac{k_p L^4}{EI^*}, \quad K_{nl} = \frac{k_{nl} L^4}{EI^*},$$

$$\eta = \frac{1}{(1 + EA\alpha T)}, \quad \bar{N}_T = \frac{N_t L^2}{EI^*}$$

By substituting  $\hat{Y}(x) = \hat{Y} e^{-i\omega x}$  into Eq. (35) we get

$$\begin{aligned} & (1 + EA\alpha T - \eta AH_x^2) \frac{\partial^4 y}{\partial x^4} \\ & + [EA\alpha T - \eta AH_x^2 + \beta - k_w + k_p + k_{nl}] \frac{\partial^2 y}{\partial x^2} \\ & + 2i\beta\rho A \frac{\partial y}{\partial x} - [\rho A + (k_w + k_p + k_{nl})] = 0 \end{aligned} \quad (37)$$

A non-trivial solution of the wave amplitude  $\bar{Y}$  implies that

$$y(x, t) = \bar{y} e^{-i k_n x} \quad (38)$$

Thus, by substituting Eq. (38) into Eq. (37), we get the following equation

$$\begin{aligned} & (1 + EA\alpha T - \eta AH_x^2) k_n^4 \\ & + [EA\alpha T - \eta a H_x^2 + \beta - (-k_w + k_p + k_{nl}) + \tau^2] k_n^2 \\ & + (2i\beta\rho A) k_n - [\rho A + (-k_w + k_p + k_{nl})] = 0 \end{aligned} \quad (39)$$

which represents the characteristic equation for a continuum structure (ECS) coupled with a surrounding medium of SWCNT.

## 5 Boundary conditions

In the following we provide an analytical solution of the governing vibration equations for a simply-supported (S-S) and clamped-clamped (C-C) nanobeam.

### 5.1 Simply supported SWCNT

For a S-S SWCNT we have to enforce the following conditions at  $(X) = (0, L)$

$$Y(x)|_{X=0} = 0, \quad (40)$$

$$M(X) = \left( -EI^* \frac{\partial^2 Y(X)}{\partial X^2} + (e_0 a)^2 \begin{bmatrix} (\rho A) \frac{\partial^2 Y(X)}{\partial t^2} + \\ q^{(mag)} \frac{\partial^2 Y(X)}{\partial X^2} - \\ f(x) \frac{\partial^2 Y(X)}{\partial X^2} + \\ EA\alpha T \frac{\partial^2 Y(X)}{\partial X^2} \end{bmatrix} \right)_{X=0} = 0,$$

$$Y(x)|_{X=L} = 0,$$

$$M(X) = \left( -EI^* \frac{\partial^2 Y(X)}{\partial X^2} + (e_0 a)^2 \begin{bmatrix} (\rho A) \frac{\partial^2 Y(X)}{\partial t^2} + \\ q^{(mag)} \frac{\partial^2 Y(X)}{\partial X^2} - \\ f(x) \frac{\partial^2 Y(X)}{\partial X^2} + \\ EA\alpha T \frac{\partial^2 Y(X)}{\partial X^2} \end{bmatrix} \right)_{X=L} = 0,$$

$$\prod(X) = \left( \begin{array}{c} - \left( EI^* \frac{\partial^3 Y}{\partial X^3} \right) + \\ \left( e_0 a \right)^2 \left[ \begin{array}{c} (\rho A) \frac{\partial^3 Y}{\partial X^2 \partial t^2} + \\ \frac{\partial^2 q^{(mag)}}{\partial X^2} - \\ \frac{\partial f(x)}{\partial X} + EA\alpha T \end{array} \right] \end{array} \right)_{X=0} = 0$$

$$Y(x)|_{X=L} = 0,$$

$$\prod(X) = \left( \begin{array}{c} - \left( EI^* \frac{\partial^3 Y}{\partial X^3} \right) \\ + \left( e_0 a \right)^2 \left[ \begin{array}{c} (\rho A) \frac{\partial^3 Y}{\partial X^2 \partial t^2} + \\ \frac{\partial^2 q^{(mag)}}{\partial X^2} - \\ \frac{\partial f(x)}{\partial X} + EA\alpha T \end{array} \right] \end{array} \right)_{X=L} = 0$$

### 5.2 Clamped - Clamped SWCNT

Let us now assume a C-C SWCNT subjected to an axial compressive load. In this case, we have to enforce the following boundary conditions

$$Y(x)|_{X=0} = 0, \quad \frac{\partial Y(X)}{\partial X} \Big|_{X=0} = 0, \quad (41)$$

$$Y(x)|_{X=L} = 0, \quad \frac{\partial Y(X)}{\partial X} \Big|_{X=L} = 0$$

## 6 Numerical results and discussion

In this section we analyse the nonlinear vibration of a SWCNT embedded in a polymer matrix subjected to a magneto-thermo-elastic force. The geometrical and material properties assumed within the numerical investigation is shown in Table 1, whose results are summarized in Tables 2-4 in terms of natural frequencies for different nonlocal constants and foundations parameters. Based on results in these tables, it is worth noticing that frequencies decrease for an increasing value of the nonlocal parameter, for both C-C and S-S boundary conditions. It is also visible that the magnitude of frequency increases, as the foun-

**Table 1:** Material properties [27, 61]

Materials	PZT
$EI$	$1.1122 \times 10^{-25} \text{ N m}^9$
$\alpha^0$	$-1.5 \times 10^{-6} \text{ C}^{-1}$
$\rho$	$2.3 \text{ g/cm}^3$
$e_0$	$0.31 \text{ nm}$
$a$	$0.142 \text{ N/m}$
$E_s$	$35.3 \text{ N/m}$
$\mu$	$4\pi \times 10^{-7} \text{ N/m}$
$H_x$	$2 \times 10^8 \text{ A/m}$

**Table 2:** Nonlocal constant and Winkler foundation effects on frequency of nanotube, ( $K_p = 0$ ), ( $K_{nl} = 0$ )

$\tau$	C – C		S – S	
	$K_w = 25$	$K_w = 50$	$K_w = 25$	$K_w = 50$
0.5	1.5142	1.5609	1.3239	1.3701
1	1.2204	1.2310	1.0926	1.0970
1.5	0.9665	0.9721	0.8442	0.8663
2	0.6416	0.6776	0.5919	0.6116
2.5	0.3633	0.3638	0.4350	0.4551

**Table 3:** Nonlocal constant and Pasternak foundation effects on frequency of nanotube ( $L/h = 10$ ), ( $K_w = 0$ ), ( $K_{nl} = 0$ )

$\tau$	C – C		S – S	
	$K_p = 25$	$K_p = 50$	$K_p = 25$	$K_p = 50$
0.5	1.5651	1.6725	1.9367	1.9583
1	1.3495	1.3576	1.8640	1.9356
1.5	1.1019	1.1117	1.8129	1.8345
2	0.9543	0.9656	0.7296	0.7712
2.5	0.7792	0.7930	0.7149	0.7188

**Table 4:** Non local constant and nonlinear foundation effects on frequency nanotube ( $L/h = 10$ ), ( $K_w = 0$ ), ( $K_p = 0$ )

$\tau$	C – C		S – S	
	$K_{nl} = 25$	$K_{nl} = 50$	$K_{nl} = 25$	$K_{nl} = 50$
0.5	1.2321	1.2541	1.1512	1.2349
1	1.1881	1.2101	0.9926	1.0704
1.5	1.2221	1.1441	0.8458	0.9177
2	1.0121	1.0141	0.7469	0.7671
2.5	0.9681	0.9901	0.6404	0.6475

dation stiffness increases. The natural frequency, for both simply and clamped supports, is computed for different thermal parameters and nonlocal values in Table 5. From results, it is observed that as the thermal parameter grows, the frequency increases but the small scale effects reduces the values of frequency for both boundary conditions. In Table 6, the natural frequency values are reported for different densities and Poisson’s ratios. As listed in Table 6, the density and Poisson’s ratio variation does not affect significantly the natural frequency (below 2%). Table 7 also presents the numerical results from a comparative study in terms of maximum transverse deflection for a C-C CNT accounting (or not) possible surface effects. Our results are in reasonable agreement with predictions from the literature, which confirms the accuracy of the proposed formulation.

**Table 5:** Natural frequency (THz) of a CNT in both local and nonlocal boundary conditions

$\tau$	$\alpha^0 = -1.5 \times 10^{-6} C^{-1}$		$\alpha^0 = -2.0 \times 10^{-6} C^{-1}$		$\alpha^0 = -2.5 \times 10^{-6} C^{-1}$	
	L.BC.	NL.BC.	L.BC.	NL.BC.	L.BC.	NL.BC.
	0	0.0180	0.0178	0.0176	0.0173	0.0259
0.5	0.0145	0.0142	0.0169	0.0167	0.0231	0.0229
1	0.0134	0.0131	0.0150	0.0148	0.0212	0.0214
1.5	0.0039	0.0027	0.0116	0.0113	0.0207	0.0205

**Table 6:** Natural frequency (THz) of a S-S CNT for different densities and Poisson’s ratios

L/R	Density			Poisson’s ratio		
	$\rho_1 = 2.16$	$\rho_2 = 2.3$	$\rho_3 = 2.7$	$\nu_1$	$\nu_2$	$\nu_3$
1	1.1634	1.0575	0.8226	1.0618	1.0604	1.0527
2	0.7977	0.7821	0.7664	0.7593	0.7554	0.7546
3	0.4114	0.4087	0.4002	0.4964	0.4924	0.4918
4	0.3498	0.3382	0.3157	0.3454	0.3453	0.3396
5	0.2539	0.2459	0.2391	0.2377	0.2374	0.2362
6	0.1913	0.1852	0.1790	0.1947	0.1931	0.1927
7	0.1513	0.1435	0.1353	0.1295	0.1287	0.1268
8	0.1435	0.1353	0.1265	0.0904	0.0863	0.0804
9	0.1171	0.1069	0.0956	0.0690	0.0633	0.0629
10	0.0976	0.0869	0.0777	0.0438	0.0432	0.0425
15	0.0828	0.0676	0.0478	0.0216	0.0213	0.0199

**Table 7:** Maximum transverse deflection in a C-C nanotube incorporating surface effects (S.E.)

(L/h)	Basutkar, <i>et al.</i> [62]		Present	
	(S. E)	(S. E $\neq$ 0)	(S. E = 0)	(S. E $\neq$ 0)
10	0.6343	0.6334	0.6396	0.6363
15	0.9472	0.9459	0.9450	0.9432
20	1.2550	1.2530	1.2934	1.2914

In Figures 4 and 5 we show the dimensionless frequency versus the dimensionless amplitude for various non-local parameters, while assuming  $L/h = 10-20$ ,  $V = 0$ ,  $K_p = 20$ ,  $\Delta T = 20^\circ$  and  $\alpha = 0.5$ . Based on the results, it is found that the dimensionless frequency increases with the amplitude. When the nonlocal parameter increases, the frequency magnitude decreases, thus revealing the importance of considering nonlocalities within such vibration problems. A softening frequency behaviour is also observed for an increased structural slenderness, as shown in Figure 5. A similar systematic investigation is, thus, repeated for different Winkler parameters, while keeping  $L/h = 10$ ,  $V = 0$ ,  $\alpha = 0.5$ ,  $K_p = 20$ ,  $\Delta T = 20^\circ$  and  $30^\circ$ , as plotted in Figures 6 and 7, respectively. All the plots in both figures, increase monotonically, where an increased Win-

kler’s parameter yields higher frequencies for each fixed dimensionless amplitude. This corresponds to an overall hardening behaviour of the structural stiffness of the nanotube.

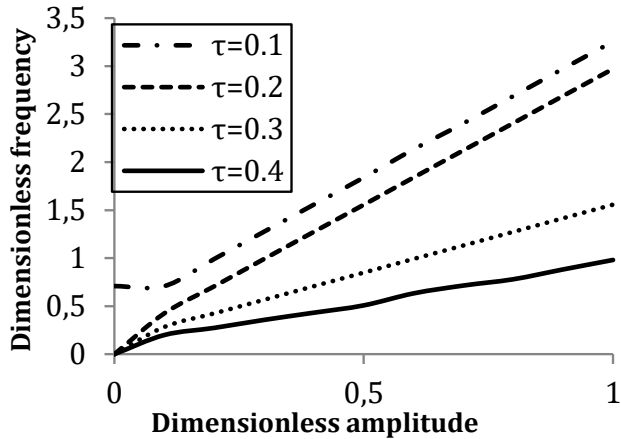


Figure 4: Dimensionless frequency vs. dimensionless amplitude for various non-local parameter. ( $L/h = 10, V = 0, K_w = K_p = 20, \Delta T = 20^\circ, \alpha = 0.5$ )

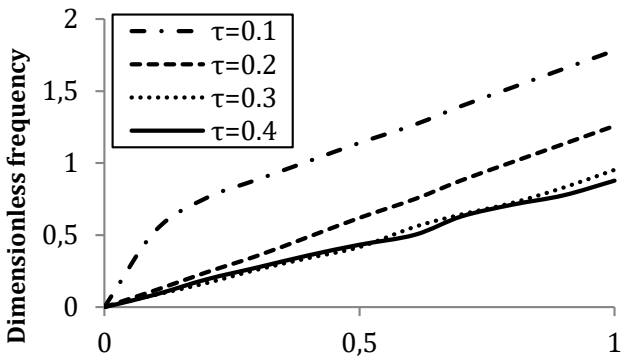


Figure 5: Dimensionless frequency vs. dimensionless amplitude for various non-local parameter. ( $L/h = 20, V = 0, K_w = K_p = 20, \Delta T = 20^\circ, \alpha = 0.5$ )

The frequency variation of the nanotube is presented in Figures 8 and 9, in dimensionless form, with respect to the amplitude for a varying voltage level, under the following assumptions:  $L/h = 10-20, \alpha = 0.5, K_p = K_w = 20-30$  and  $\Delta T = 20^\circ$ . It is found that an increased amplitude gets higher frequencies, whose variation is strictly dependent on the applied voltage. An axial tensile or compressive force is produced within the nanotube by applying a positive or negative voltage, respectively. It is also found that the dimensionless frequency is slightly dependent on

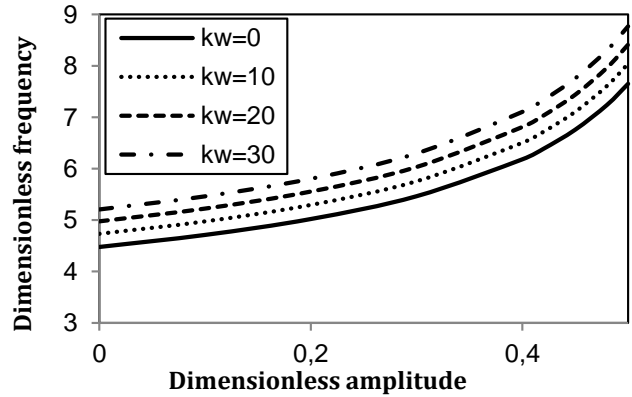


Figure 6: Dimensionless frequency vs. dimensionless amplitude for different foundation parameter values. ( $L/h = 10, V = 5, K_p = 20, \Delta T = 20^\circ, \alpha = 0.5$ )

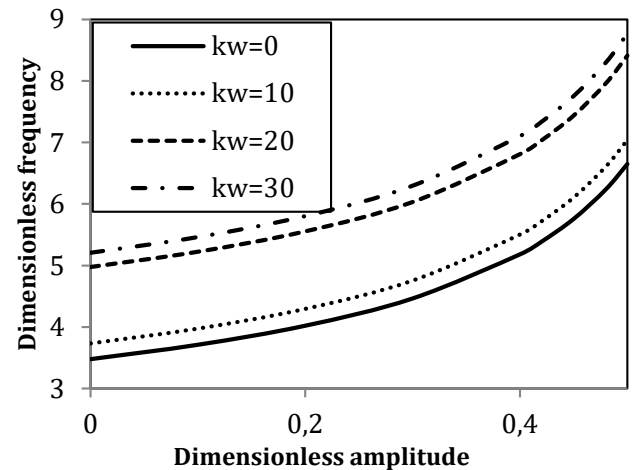


Figure 7: Dimensionless frequency vs. dimensionless amplitude for different Pasternak foundation values. ( $L/h = 10, V = 5, K_p = 20, \Delta T = 30^\circ, \alpha = 0.5$ )

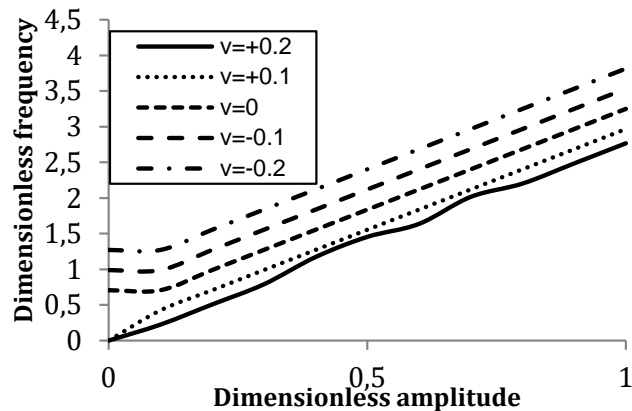
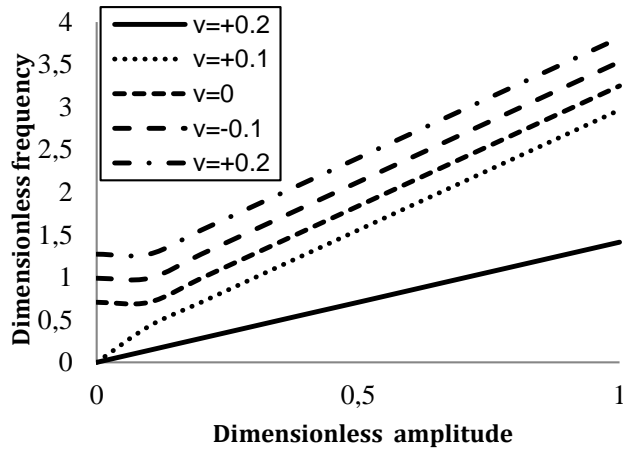
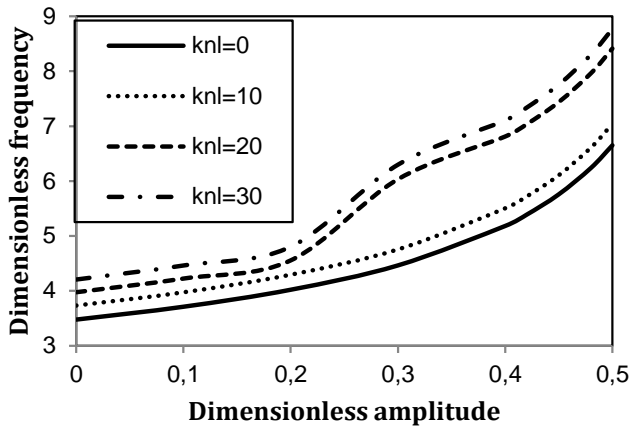


Figure 8: Dimensionless frequency vs. dimensionless amplitude for different electric voltages. ( $L/h = 10, K_w = K_p = 20, \Delta T = 20^\circ, \alpha = 0.5$ )



**Figure 9:** Dimensionless frequency vs. dimensionless amplitude for various for various electric voltages. ( $L/h = 20, K_w = K_p = 30, \Delta T = 20^\circ, \alpha = 0.5$ )



**Figure 10:** Dimensionless frequency vs. dimensionless amplitude for different nonlinear foundation values. ( $L/h = 10, V = 0, K_w = K_p = 10, \Delta T = 10^\circ, \alpha = 0.5$ )

the slenderness ratio and foundation parameter, under a fixed temperature  $\Delta T = 20^\circ$ . The effect of the frequency vs. amplitude for the nanotube is plotted in dimensionless form in Figures 10 and 11, for a different nonlinear foundation parameter, and for fixed values of  $L/h = 10-20, K_p = K_w = 20-30$  and  $\Delta T = 20^\circ$ . One can observe that the dimensionless frequency increases in a wave propagation trend for an increasing amplitude, when  $L/h = 10$ , and  $K_p = K_w = 20$ . Moreover, the frequency increases with the oscillation modes, for increased values of slenderness and foundation parameters.

Figures 12 and 13 also depict the bending moment response for the first three modes along the nanotube length, while assuming  $L/h = 10, V = 0, \alpha = 0.5, K_w = K_p = 20, \Delta T = 20^\circ, \Delta H = 10$ . Based on the plots in these two figures, it is worth noticing that, as the length grows, the

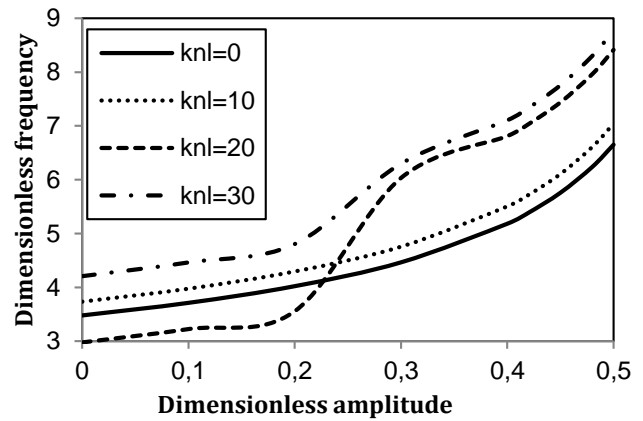


**Figure 11:** Dimensionless frequency vs. dimensionless amplitude for different nonlinear foundations. ( $L/h = 20, V = 0, K_w = K_p = 20, \Delta T = 20^\circ, \alpha = 0.5$ )

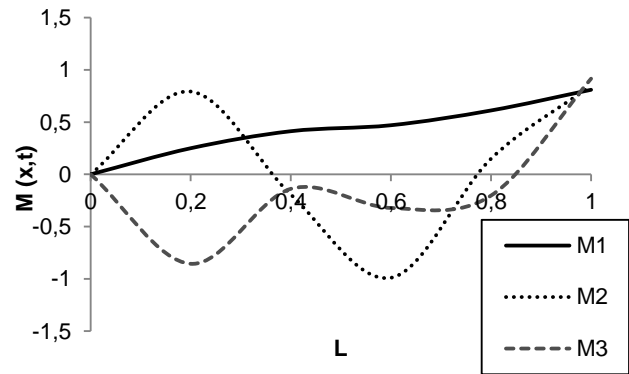


**Figure 12:** Bending moment vs. length for different modes. ( $L/h = 10, V = 0, K_w = K_p = 20, \Delta T = 20^\circ, \Delta H = 10, \alpha = 0.5$ )

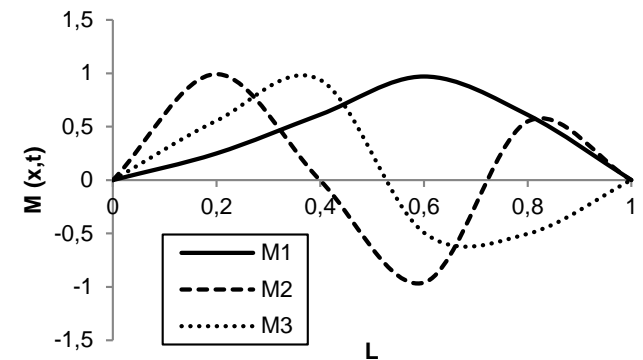


**Figure 13:** Bending moment vs. length for different modes. ( $L/h = 10, V = 0, K_w = K_p = 20, \Delta T = 20^\circ, \Delta H = 20, \alpha = 0.5$ )

bending moment attains a tensile and compressive nature when moving versus higher modes. The influence of the magnetic field is also clearly observable in the wave trend. Figures 14 and 15 present the dimensionless frequency vs. the attached mass ratio, for  $L/h = 10, V = 0.2, K_w =$

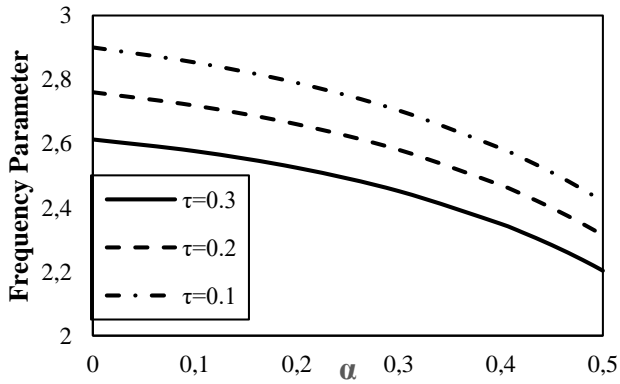


Figure 14: Dimensionless frequency vs. attached mass ratio. ( $L/h = 10$ ,  $V = 0.2$ ,  $K_w K_p = 20$ ,  $\Delta T = 10^\circ$ ,  $\Delta H = 10$ )

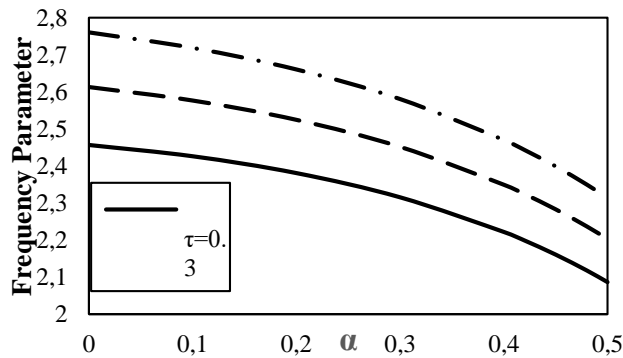


Figure 15: Dimensionless frequency vs. attached mass ratio. ( $L/h = 10$ ,  $V = 0.2$ ,  $K_w = K_p = 20$ ,  $\Delta T = 20^\circ$ ,  $\Delta H = 20$ )

$K_p = 20$ , and for different environmental conditions,  $(\Delta T, \Delta C) = (10,10)$ ,  $(20,20)$ , respectively. It is seen that the frequency parameter decreases as the attached mass ratio values increases. It should be also pointed out that thermal and hygro-thermal environment degrades the plate stiffness for an increased mass ratio. Moreover, it is found that the effects of a varying temperature and moisture concentration, are more pronounced at lower mass ratios. Generally, by attaching a particle on a SWCNT, the total mass of the system amplifies although the stiffness remains unchanged, with a consequent decreased frequency. As far as the nonlocal effect is concerned, we can finally observe that an increasing nonlocal parameter decreases the frequency response of the structure, along with its stiffness.

## 7 Conclusion

This paper studies the nonlinear magneto-thermo-elastic waves in an armchair SWCNT resting on a polymer matrix via an Euler beam theory and the Eringen's nonlocal elas-

ticity assumptions to account for small scale effects. The ultrasonic wave dispersion problem is defined and solved theoretically, where a parametric investigation checks for the influence of the magneto-electro-mechanical loading, nonlocal parameter, and aspect ratio, on the deflection response of nanotubes. Based on the results from the systematic study, the main conclusions can be summarized as follows:

- The nonlocal scaling constant amplifies the natural frequencies of CNTs.
- An increased foundation parameter enhances the stiffness and frequency of the nanostructure, especially when assuming clamped boundary conditions.
- Armchair CNTs embedded in an elastic foundation, feature an improved dynamic behavior. Moreover, the Pasternak parameter affects the structural response more significantly than a Winkler-type foundation.
- The natural frequency variation between local and non local boundary conditions, maintains below 1%, in presence of thermal coefficients.
- The vibration modes of SWCNT are softened by an attached mass and for small length scale values.
- The results from this work can be useful benchmarks for the study and design of nanodevices that make use of the wave propagation properties of armchair SWCNTs embedded on a polymer matrix, i.e. nano-oscillators, micro wave absorbing, nano-electron technology and nano-electro-magneto-mechanical systems (NEMMS).

## References

- [1] Ebrahimi, F., Dabbagh, A., Magnetic field effects on thermally affected propagation of acoustical waves in rotary double-nanobeam systems, *Waves Random Complex Medium*, 2018, 1–21.
- [2] Wang, Q., Wave propagation in carbon nanotubes via nonlocal continuum mechanics, *J. Appl. Phys.*, 2005, 98, 124301–6.
- [3] Heirechea, H., Tounsi, A., Benzaira, A., Maachoua M.E.A., Adda Bedia, E.A.A. Sound wave propagation in single-walled carbon nanotubes using nonlocal elasticity, *Physica E Low Dimens. Syst. Nanostruct.*, 2008, 40, 2791–2799.
- [4] Eringen, A.C., *Nonlocal continuum field theories*, Springer, Berlin, 2002.
- [5] Eringen, A.C., Edelen, D.G.B., On nonlocal elasticity, *Int. J. Eng.*, 1972, 10(3), 233–248.
- [6] Eringen, A.C., On differential equation of nonlocal elasticity and solution of screw dislocation and surface waves, *J. Appl. Phys.*, 1983, 55, 4703.

- [7] Wang, L., Hu, H., Guo, W., Validation of the non-local elastic shell model for studying longitudinal waves in single-walled carbon nanotubes, *Nanotechnol.*, 2006, 17,1408–1415.
- [8] Fang, B., Nonlinear vibration analysis of double-walled carbon nanotubes based on nonlocal elasticity theory, *Appl. Math. Model.*, 2013, 37(3), 1098–1107.
- [9] Saadatnia, Z., Esmailzadeh, E., Nonlinear harmonic vibration analysis of fluid-conveying piezoelectric-layered Nanotubes, *Compos. B. Eng.*, 2017, 123, 193–209.
- [10] Askari, H., Esmailzadeh, E., Forced vibration of fluid conveying carbon nanotubes considering thermal effect and nonlinear foundations, *Compos. B. Eng.*, 2017, 113, 31–43.
- [11] Gheshlaghi, B., Hasheminejad, S.M., Surface effects on nonlinear free vibration of nanobeams, *Compos. B. Eng.*, 2011, 42(4), 934–937.
- [12] Sadeghi-Goughari, M., Jeon, S., Kwon, H., Effects of magnetic-fluid flow on structural instability of a carbon nanotube conveying nanoflow under a longitudinal magnetic field, *Phys. Lett. A*, 2017, 381, 35, 2898–905.
- [13] Zhen, Y.X., Wen, S.L., Tang, Y., Free vibration analysis of viscoelastic nanotubes under longitudinal magnetic field based on nonlocal strain gradient Timoshenko beam model, *Physica E Low Dimens. Syst. Nanostruct.*, 2019, 105, 116–124.
- [14] Dai, H.L., Ceballes, S.A., Abdelkefi, A.Y.Z., Hong, Y.Z., Wang, L., Exact modes for post buckling characteristics of nonlocal nanobeams in a longitudinal magnetic field, *Appl. Math. Model.*, 2018, 55, 758–775.
- [15] Ebrahimi, F., Barati, M.R., Vibration analysis of piezoelectrically actuated curved nanosize FG beams via a nonlocal strain electric field gradient theory, *Mech. Adv. Mater.*, 2018, 25(4), 350–359.
- [16] Li, L., Yujin Hu, L., Ling, L., Wave propagation in viscoelastic single-walled carbon nanotubes with surface effect under magnetic field based on nonlocal strain gradient theory, *Physica E Low Dimens. Syst. Nanostruct.*, 2016, 75, 118–124.
- [17] Arani, A.G., Roudbari, M.A., Amir, S., Longitudinal magnetic field effect on wave propagation of fluid-conveyed SWCNT using Knudsen number and surface considerations, *Appl. Math. Model.*, 2016, 40, 2025–2038.
- [18] Zhang, D.P., Lei Y., Shen, Z.B., Vibration analysis of horn-shaped single-walled carbon nanotubes embedded in viscoelastic medium under a longitudinal magnetic field, *Int. J. Mech.*, 2016, 118, 219–230.
- [19] Güven, U., General investigation for longitudinal wave propagation under magnetic field effect via nonlocal elasticity, *Appl. Math. Mech-Engl.*, 2015, 36, 1305–1318.
- [20] Wang, Q., Varadan, V.K., Quek, S.T., Small scale effect on elastic buckling of carbon Nanotubes with nonlocal continuum models, *Phys. Lett. A.*, 2006, 357, 130–135.
- [21] Azarboni, H.R., Magneto - thermal primary frequency response analysis of carbon nanotube considering surface effect under different boundary conditions, *Compos. B. Eng.*, 2019, 165, 435–441.
- [22] Pradhan, S.C., Phadikar, J.K., Small scale effect on vibration of embedded multilayered graphene sheets based on nonlocal continuum models, *Phys. Lett. A.*, 2009, 373, 1062–1069.
- [23] Semmah, A., Anwar, B.O., Mahmoud, S.R., Houari, H., Tounsi, A., Thermal buckling properties of zigzag single-walled carbon nanotubes using a refined nonlocal model, *Adv. Mat. Res.*, 2014, 3(2), 77–89.
- [24] Naceri, M., Zidour, M., Semmah, A., Houari, M.S.A., Benzair, A., A. Tounsi, A., Sound wave propagation in armchair single walled carbon nanotubes under thermal environment, *J. Appl. Phys.*, 2011, 110, 124322.
- [25] Baghdadi, H., Tounsi, A., Zidour, M., Benzair, A., Thermal Effect on Vibration Characteristics of Armchair and Zigzag Single-Walled Carbon Nanotubes Using Nonlocal Parabolic Beam Theory, *Fuller. Nanotub. Car. N.*, 2014, 23, 266–272.
- [26] Benzair, A., Tounsi, A., Besseghier, A., Heireche, A., Moulay, N., Boumia, L., The thermal effect on vibration of single-walled carbon nanotubes using nonlocal Timoshenko beam theory, *J. Phys. D.*, 2008, 41, 225404, 1–10.
- [27] Besseghier, A., Tounsi, A., Houari, M.S.A., Benzair, A., Boumia, L., Heireche, H., Thermal effect on wave propagation in double-walled carbon nanotubes embedded in a polymer matrix using nonlocal elasticity, *Physica E Low. Dimens.*, 2011, 43, 1379–1386.
- [28] Zhang, Y.O., Liu, X., Liu, R. G., Thermal effect on transverse vibrations of double walled carbon nanotubes, *Nanotechnol.*, 2007, 18, 445701-7.
- [29] Lata, P., Kaur, I., Thermo mechanical interactions in a transversely isotropic magneto thermo-elastic solids with two temperature and rotation due to time harmonic sources, *Coupled Syst. Mech.*, 2019, 8(3), 219–245.
- [30] Lata, P., Kaur, I., Transversely isotropic thick plate with two temperature and GN type-III in frequency domain, *Coupled Syst. Mech.*, 2019, 8(1), 55–70.
- [31] Lata, P., Kumar, R., Sharma, N., Plane waves in anisotropic thermo-elastic medium, *Steel Compos. Struct.*, 2016,22(3), 567–587.
- [32] Kumar, R., Sharma, N., Lata, P., Abo-Dahab, S.M., Rayleigh waves in anisotropic magneto thermo-elastic medium, *Coupled. Syst. Mech.*, 2017, 6(3), 317–333.
- [33] Narendar, S., Roy Mahapatra D., Gopalakrishnan, S., Prediction of nonlocal scaling parameter for armchair and zigzag single-walled carbon nanotubes based on molecular structural mechanics, nonlocal elasticity and wave propagation, *Int. J. Eng. Sci.*, 2011, 49(6), 509–522.
- [34] Adda Bedia, W., Benzair, A., Semmah, A., Tounsi, T., Mahmoud, S.R. On the Thermal Buckling Characteristics of Armchair Single-Walled Carbon Nanotube Embedded in an Elastic Medium Based on Nonlocal Continuum Elasticity, *Braz. J. Phys.*, 2015, 45, 225–233.
- [35] Zidour, M., Daouadji, T.H., Benrahou, K.H., Tounsi, A., Adda Bedia, E.A., Hadji, L., Buckling analysis of chiral single-walled carbon nanotubes by using the nonlocal Timoshenko beam theory, *Mech. Compos.*, 2014, 50(1), 95–104.
- [36] Bensattallah, T., Daouadji, T.H., M. Zidour, M., Tounsi, A., Adda Bedia, E.A.A., Investigation of thermal and chirality effects on vibration of single-walled carbon nanotubes embedded in a polymeric matrix using nonlocal elasticity theories, *Mech. Compos.*, 2016, 52(4), 555–568.
- [37] Hsu, J.C., Chang, R.P., Chang, W.J., Resonance frequency of Chiral single walled carbon nanotubes using Timoshenko beam theory, *Phys. Lett. A*, 2008, 373, 2757–2759.
- [38] Aydogdu, M., Axial vibration analysis of nanorods(carbon nanotubes) embedded in an elastic medium using nonlocal elasticity, *Mech. Res. Commun.*, 2012, 43, 34–40.
- [39] Ansari, R., Gholami, R., Sahmani, S., On the dynamic stability of embedded single-walled carbon nanotubes including thermal environment effects, *Sci. Iranica*, 2012, 19(3), 919–925.

- [40] Arefi, M., Bidgoli, E.M.-R., Dimitri, R., Tornabene, F., Reddy, J.N., Size-dependent free vibrations of FG polymer composite curved nanobeams reinforced with graphene nanoplatelets resting on Pasternak foundations, *Appl. Sci.*, 2019, 9(8),1580.
- [41] Malikan, M., Nguyen, V.B., Dimitri, R., Tornabene, F., Dynamic modeling of non-cylindrical curved viscoelastic single-walled carbon nanotubes based on the second gradient theory, *Mater. Res. Expr.*, 2019, 6(7), 07504.
- [42] Nejati, M., Ghasemi-Ghalebahman, A., Soltanmaleki, A., Dimitri, R., Tornabene, F., Thermal vibration analysis of SMA hybrid composite double curved sandwich panels, *Comp. Struct.*, 2019, 224, 111035.
- [43] Heydarpour, Y., Malekzadeh, P., Dimitri, R., Tornabene, F., Thermoelastic analysis of functionally graded cylindrical panels with piezoelectric layers, *Appl. Sci.*, 2020, 10(4), 1397.
- [44] Karimi, M., Khorshidi, K., Dimitri, R., Tornabene, F., Size-dependent hydroelastic vibration of FG microplates partially in contact with a fluid, *Compos. Struct.*, 2020, 244, 112320.
- [45] Sedighi, H.M., Ouakad, H.M., Dimitri, R., Tornabene, F., Stress-driven nonlocal elasticity for the instability analysis of fluid-conveying C-BN hybrid-nanotube in a magneto-thermal environment, *Physica Scripta*, 2020, 95(6), 065204.
- [46] Wu, D.H., Chien, W.T., Chen, C.S., Chen, H.H., Resonant frequency analysis of fixed-free single-walled carbon nanotube-based mass sensor, *Sens. Actuators A Phys.*, 2006, 126,(1),117–121.
- [47] Li, C., Chou, T.W., Atomistic Modeling of Carbon Nanotube-based Mechanical Sensors, *J. Intell. Mater. System Struct.*, 2006, 17, 244–254.
- [48] Barati, M.R., Shahverdi, H., Frequency analysis of nanoporous mass sensors based on a vibrating heterogeneous nanoplate and nonlocal strain gradient theory, *Microsyst. Technol.*, 2018, 24, 1479–1494.
- [49] Chowdhury, R., Adhikari, S., Mitchell, J., Vibrating carbon nanotube based bio-sensors, *Physica E Low Dimens. Syst. Nanostruct.*, 2009, 42, 104–109.
- [50] Arda, M., Aydogdu, M., Vibration analysis of carbon nanotube mass sensors considering both inertia and stiffness of the detected mass, *Mech. Based Des. Struct. Mach.*, 2020, 1–17.
- [51] Liu, H., Lyu, Z., Modeling of novel nanoscale mass sensor made of smart FG magneto-electro-elastic nanofilm integrated with graphene layers, *Thin-Walled Struct.*, 2020,151, 106749.
- [52] Lee, H.L., Hsu, J.C., Chang, W.J., Frequency Shift of Carbon-Nanotube-Based Mass Sensor Using Nonlocal Elasticity Theory, *Nanoscale. Res. Lett.* 2010, 5, 1774–1778.
- [53] Nematollahi, M.A., Jamali, B., Hosseini, M., Fluid velocity and mass ratio identification of piezoelectric nanotube conveying fluid using inverse analysis, *Acta Mech.*, 2019, 231, 683–676.
- [54] Aydogdu, M., Filiz, S., Modeling carbon nanotube-based mass sensors using axial vibration and nonlocal elasticity, *Physica E*, 2011,43,1229–1234.
- [55] Tokio, Y., Recent development of carbon nanotube, *Synth. Met.*, 1995, 70, 1511–1518.
- [56] Wu, Y., Zhang, X., Leung, A.Y.T., Zhong, W., An energy-equivalent model on studying the mechanical properties of single-walled carbon nanotubes, *Thin-Walled. Struct.*, 2006, 44, 667–676.
- [57] Lei, X.W., Natsuki, T., Shi, J.X., Ni, Q.Q., Surface effects on the vibrational frequency of double-walled carbon nanotubes using the nonlocal Timoshenko beam model, *Compos. B. Eng.*, 2012, 43, 64–69.
- [58] Yan, Z., Jiang, L., The Vibrational and Buckling Behaviors of Piezoelectric Nanobeams with Surface Effects, *Nanotechnol.*, 2011, 22(24), 245703.
- [59] Barati, M.R., Investigating nonlinear vibration of closed circuit flexoelectric nanobeams with surface effects via hamiltonian method, *Microsyst. Technol.*, 2018, 24, 1841–1851.
- [60] Narender, S., Gopalakrishnan, S., Ultrasonic wave charenterstics of a nanorods via nonlocal strain gradient models, *J. Appl. Phys.*, 2010,107,084312.
- [61] Lee, L. H., Chang, W. J., Vibration analysis of a viscous-fluid-conveying single-walled carbon nanotube embedded in an elastic medium, *Physica E Low Dimens. Syst. Nanostruct.*, 2009, 41, 529–53.
- [62] Basutkar, R. Sidhardh, S., Ray, M.C., Static analysis of flexoelectric nanobeams incorporating surface effects using element free Galerkin method, *Eur. J. Mech. A-Solid.*, 2019, 76,13–24.